Spanish Journal of Agricultural Research
20 (1), e0203, 12 pages (2022)
eISSN: 2171-9292
https://doi.org/10.5424/sjar/2022201-17138
INIA-CSIC

RESEARCH ARTICLE

OPEN ACCESS

Assessment of consumer-grade camera-derived vegetation indices for monitoring nitrogen and leaf relative water content of maize

Fatemeh Mousabeygi[1], Samira Akhavan[1] and Yousef Rezaei[2]

[1] *Bu-Ali Sina University, Faculty of Agriculture, Dept. Water Engineering, Hamedan, Iran* [2] *Bu-Ali Sina University, Faculty of Engineering, Dept. Civil Engineering, Hamedan, Iran*

Abstract

Aim of study: To develop non-destructive and rapid monitoring of water and nitrogen status in maize crops.

Area of study: Bu-ali Sina University, Hamedan province, Iran.

Material and methods: We used a low-cost modified consumer-grade camera to extract 40 vegetation indices for monitoring leaf N concentrations, SPAD values and relative water content (RWC). In this regard, 528 images taken by the low-cost camera in two consecutive years (2017 and 2018) from maize plants cultivated in a greenhouse under different irrigation and N treatments were evaluated.

Main results: Results showed that the best performance outcomes regarding the studied vegetation indices were MCARI, CTVI and CR for SPAD values; MCARI, HUE and CTVI for leaf N concentrations; and TRVI, NDVI and DVI for RWC. In order to increase accuracy of estimated measured data, multiple linear regression equations with combinations of the MCARI, TRVI, NDVI and EVI indices were used. As observed, R^2 value was 0.91, 0.60 and 0.90 for SPAD, leaf N concentration and RWC estimation, respectively.

Research highlights: The combination of MCARI, TRVI, NDVI and EVI indices provided more accuracy to most of the previous single variable regression models.

Additional key words: vegetation index; digital camera; leaf nitrogen concentration; *Zea mays* L.

Abbreviations used: CCD (charge coupled device); CMOS (complementary metal oxide semiconductor); DAS (day after sowing); EXG (Excess Green); I (irrigation); IR (infrared); LAI (leaf area index); LARS (low altitude remote sensing); MBE (mean bias error); NIR (near-infrared); RGB (red, green, and blue bands); RMSE (root mean square error); RWC (relative water content); RS (remote sensing).

Authors' contributions: Conceived, designed and performed the experiments and analysed the data: FM. Contributed materials/analysis tools and wrote the paper: FM, SA, YR. Critical revision of the manuscript: SA, YR.

Citation: Mousabeygi, F; Akhavan, S; Rezaei, Y (2022). Assessment of consumer-grade camera-derived vegetation indices for monitoring nitrogen and leaf relative water content of maize. Spanish Journal of Agricultural Research, Volume 20, Issue 1, e0203. https://doi.org/10.5424/sjar/2022201-17138.

Supplementary material (Tables S1, S2 and S3) accompanies the paper on SJAR's website

Received: 04 Jul 2020. **Accepted:** 28 Jan 2022.

Funding: The authors received no specific funding for this work.

Competing interests: The authors have declared that no competing interests exist.

Correspondence should be addressed to Samira Akhavan: akhavan_samira@yahoo.com

Introduction

Iran is the second largest country in the Middle East, most parts of which have arid and semi-arid climates (Akhavan *et al.*, 2018). So, like the other arid and semi-arid regions of the world, Iran is experiencing water deficit currently. Nevertheless, 12 million hectares are cultivated in Iran, approximately 380,000 of which are under maize cultivation (Ahmadi, 2017). Maize productivity largely depends on irrigation and fertilization. Nitrogen is one of the most important fertilizers, changing the plant yield both quantitatively and qualitatively (Swain *et al.*, 2010). Nitrogen is fundamental for to photosynthesis process due to the key role it plays in producing chlorophyll. Therefore, insufficient N supply leads to smaller leaves, lower chlorophyll content and less biomass production (Prasertsak & Fukai, 1997; Yao *et al.*, 2013) so that farmers have to increase the amount of N fertilizers. Conversely, excessive N application is more costly and results in environmental problems such as water and atmospheric pollution (Kaushal *et al.*, 2011). Consequently, it is important to manage and balance maize requirements of water and N, which provide economical and environmental benefits. For irrigated production systems, the first step to optimize water use and improve N management is monitoring the plant water and N statuses.

In measuring plant water status, lowered one is usually considered the result of the soil water deficit. So, the plant water status provides an integrated view of the plant-soil progression (Dhillon *et al.*, 2014). On the other hand, water stress can be detected by plant-based measurement methods such as leaf stomatal conductance, leaf water status, relative water content (RWC), leaf area analysis and stem water potential, which are destructive and time-consuming (Pu *et al.*, 2003; Maki *et al.*, 2004). Non-destructive techniques can be used as alternatives in order to overcome abovementioned drawbacks. Under water stress, plant leaves display higher leaf temperature and chlorophyll fluorescence. Therefore, an infrared thermographic camera, and a fluorescence imaging system measure canopy temperature and photosynthetic activity of leaves, respectively, since these instruments have the potential to detect water stress (Romano *et al.*, 2011; Ballester *et al.*, 2013). Other techniques used to assess plant water are hyperspectral, multispectral and digital imaging techniques that are non-destructive and have a great value to calculate indices from spectral bands for crop water detection (Kim *et al.*, 2011).

In addition, there are two types of methods known to obtain the N status of a plant: destructive and non-destructive methods. Destructive methods are based on tissue analysis such as Kjeldahl (1883) and Dumas (1831) techniques, which have been used as a reference to estimate plant N status, but they are time-consuming analyses requiring skilled operators (Muñoz-Huerta *et al.*, 2013; Saberioon *et al.*, 2014). So, non-destructive methods have been developed to avoid these disadvantages. Several studies have reported on optical properties indicating high correlations between optical parameters and N content of the plants such as SPAD chlorophyll meter, Green seeker and Dualex and Crop Circle (Guo *et al.*, 2008; Cao *et al.*, 2013a, b). Although these instruments are expensive, they are faster than lab procedures. Remote sensing (RS) is a cost-effective alternative for estimating plant N status (Muñoz-Huerta *et al.*, 2013). This method is mainly based on satellite and aerial platforms. Although satellite platforms are used for monitoring and determining the status of nutrients in crops and their capabilities have been confirmed (Zhang *et al.*, 2006), they have such limitations as high costs of high special resolution images, limited availability of usable data (because clouds and cloud shadows may hide ground features), low temporal resolution and fixed schedule. To avoid these disadvantages, airborne sensors are used to assess nutrients status (Inoue *et al.*, 2012). However, this type of photography is still costly when specialized movements of the aircraft are required (Saberioon *et al.*, 2014). In airborne and satellite-based RS applications, remotely sensed data comes from a collection of visible and infrared portions of electromagnetic spectra. By these multispectral and hyperspectral RS data, biophysical characteristics of vegetation can be derived. But the cost of these systems is a limiting factor. A new concept of RS data acquisition is low altitude remote sensing (LARS). LARS uses various platforms such as unmanned helicopters, quadcopters, unmanned aerial planes, tractor-driven crane mounted systems, etc. All of these platforms are equipped with a film camera or a digital camera to provide crop details with higher spatial and temporal resolution (Swain *et al.*, 2010; Samseemoung *et al.*, 2012).

Recently, consumer-grade cameras have been designed to acquire images from small areas, having such advantages as low cost and high spatial resolution so that images can be easily and rapidly captured. Digital cameras recording red, green, and blue (RGB) colors channel (Zhang *et al.*, 2016) and store incoming radiance as a digital number from 0 to 225 (Ritchie *et al.*, 2008). Digital cameras are based on charge coupled devices (CCDs) or complementary metal oxide semiconductor (CMOS) sensors (Zhang *et al.*, 2016). Another type are the modified consumer-grade cameras. They are generally obtained by replacing the near-infrared (NIR)-blocking filter in front of CMOSs or CCDs with a long-pass NIR filter (Yang *et al.*, 2014). Most RS sensors include NIR detection, but high cost and complexity of the imaging system limit their utility and availability (Ritchie *et al.*, 2008). Therefore, very detailed spectral information can be obtained by using low-cost modified cameras to capture NIR light.

According to these contents, such tools are needed to make it possible to monitor crop water and N statuses at low cost. Although a number of studies have focused on and evaluated the use of modified cameras using different image processing methods (Geelen *et al.*, 2017; Cao *et al.*, 2018; de Oca *et al.*, 2018; Khan *et al.*, 2018; Zheng *et al.*, 2018; Monno *et al.*, 2019), studies that exploit a comprehensive vegetation index from low-cost modified cameras using external filters are still lacking. Use of internal filters requires specialized skills to open and remove/replace sensors, but external filters are easy to use without any need to open sensors (Putra & Soni, 2017). In our study, a low-cost modified camera and external filters including RGB and NIR spectrum wavebands were used to collect images of maize plants cultivated in a greenhouse under different irrigation and N treatments. Our objectives were to: (i) explore differences among extracted vegetation indices in response to irrigation treatments and N variations, (ii) clarify their correlations with leaf N concentration, RWC value and SPAD-502 chlorophyll meter readings, and (iii) construct a prediction model for leaf N concentration, RWC value and SPAD-502 chlorophyll meter readings. Anticipated results guided the selection of proper vegetation indices to initiate development of a non-destructive and rapid method monitoring water and N statuses in maize crop.

Material and methods

Experimental site and crop management

Field experiments were conducted during 2017 and 2018 using an early maturing variety of maize (*Zea mays* L.) in a greenhouse located in western region (34°47′60"

N, 48°28′54" E) of Iran. The experiment was planned with randomized complete block design with three replicates. Four irrigation treatments (I_1: 100% (control), I_2: 80%, I_3: 60%, and I_4: 40% of field capacity) and also four N treatments (N1: without N (control), N2: 100 kg N/ha, and N3: 200 kg N/ha and N4: 300 kg N/ha) applied as urea (46% N)) were applied. For both full-season studies, maize seeds were sown in pot containers with 30-cm diameter, 20-cm height, and 18.38-L capacity. The pot substrate was made by loam soil and plant nutrient content. Chemical and physical properties of the two types of soil (2017 and 2018) were assessed and presented in Table 1. Level of nutrients available in the soil and the kinds and amounts of supplemental fertilizer needed were determined by soil testing. Nitrogen is very susceptible to being lost from soil, therefore, split N application improves N use efficiency. Accordingly, N fertilizer was applied in four growth stages (the second irrigation, second to sixth leaf collar (V_2 to V_6), tenth leaf collar (V_{10}) and tasselling). Duration of growth stages (days) of maize in 2017 and 2018 is shown in Table S3 [suppl]. For this study, irrigation volume for a plant in a pot was calculated based on field capacity. Consequently, a soil moisture meter (LUTRON PMS-714) was used to analyse soil moisture daily. Total amounts of irrigation water applied, plant height, and leaf area index were measured. The leaf area was estimated by Planimetric method (Daughtry, 1990). The first experiment was conducted in August 2017, the second in late June /early July 2018, and harvesting date was 96 and 81 day after sowing (DAS) for 2017 and 2018, respectively. Plants emerged approximately two weeks prior to initiation of experiments. Implementation of experiments was set at the time when the fourth leaf collar emerged (V4). Hereafter, during the field growing period, leaf area and plant height were measured several times. Along with these measurements, we read chlorophyll values by a portable chlorophyll meter (SPAD 502) and took visible and infrared images 42, 52, 63 and 71 DAS in 2017, and also 23, 27, 36, 43, 48, 55 and 61 DAS in 2018. All measurements were taken between 08:00 to 11:00 a.m. SPAD readings were taken on the youngest fully expanded leaf (Zhang *et al.*, 2008; Ziadi *et al.*, 2008) and the ear leaf after tasseling (Hawkins *et al.*, 2007). For each plant, five chlorophyll meter readings were obtained. Then, the average of five readings was taken as the chlorophyll meter measurement of the plant. After these measurements, one leaf of each plants was cut using scissors; then, leaf N content (measurements by Kjeldahl method) and RWC (measurements by relative turgidity method) were calculated for each plant sample.

Table 1. Physical and chemical properties of soil

Soil variable [a]	Year	
	2017	2018
N (mg/L)	0.1	0.18
P (mg/L)	13.35	10.1
K (mg/L)	189	205
OC (%)	1.33	1.95
TNV (%)	10	8
pH	7.74	7.32
SP (%)	29.4	35
EC (µs/m)	21.9	17.4
Soil texture	Loam	Loam
Clay (%)	25.04	20.01
Silt (%)	42.72	38.41
Sand (%)	32.24	41.58

[a] OC: organic carbon. TNV: total neutralizing value. SP: saturation percentage

Obtaining the image data and vegetation indices

Figure 1 shows a simple processing workflow for extracting plant indices from RGB and infrared (IR) images of maize for this research, some equipment and plants grown during the experiments. Accordingly, a Canon® PowerShot A720 IS digital camera (8 Megapixel CCD sensors) was modified to detect radiations on additional spectral bands. The camera held by a tripod was placed in front of each pot so that its lens was not perpendicular to the pot, having approx. a 45º angle. Afterwards, we used combined IR blocking and IR filters on the front of the lens. IR filter (GREEN.L 67mm IR 720) prevented visible light from passing through while only allowing IR light to strike our camera’s sensor, and UV/IR cut filter (NightSky UV/IR Cut 2" Filter) blocked UV and IR rays. This filter cuts out IR rays above 700 nm and retains visible light spectrum. These two circular filters were attached to the front of camera lens. After taking the image using the IR filter, it was separated from the lens and UV/IR cut filter was placed on the front of the lens to take photos. When the filters were replaced, maximum effort was made to prevent the camera from being dislocated. It should be noted that a black backdrop was used during shooting in order to simplify the next procedure.

We also took steps to perform image processing (Fig. 2). For this purpose, first, we registered visible and infrared images using MATLAB R2017a (vers 9.2). Image registration algorithm is shown in Fig. 3. In the next step, four RGB and NIR bands of two images were considered for layer stacking. The next task was background elimination utilizing three components (RGB) of the image to calculate combined 2G-R-B Excess Green (EXG) used to separate green plants from background (Woebbecke *et al.*, 1995). As shown in Fig. 4, we used EXG to produce a binary mask to segment the green plants against the background. In the following step, 40 spectral indices

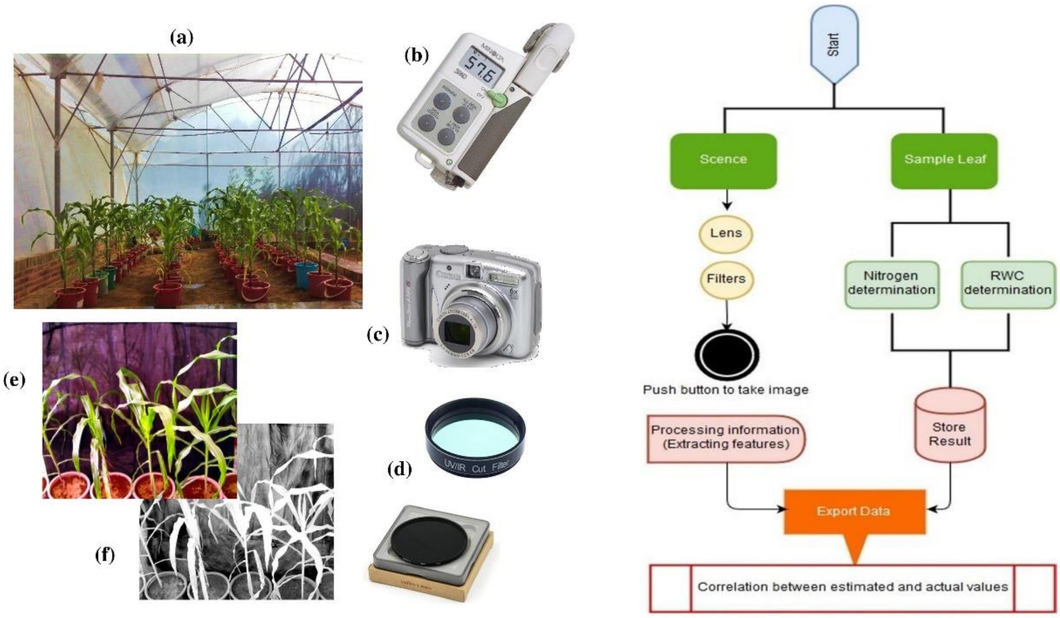

Figure 1. Right: Schematic overview of the procedure to research. Left: Side view of plants grown during the experiment (a); SPAD 502 chlorophyll meter (b); Canon® PowerShot A720 IS digital camera (c); external filters (d); RGB image of maize plants (e); and NIR image of maize plants (f).

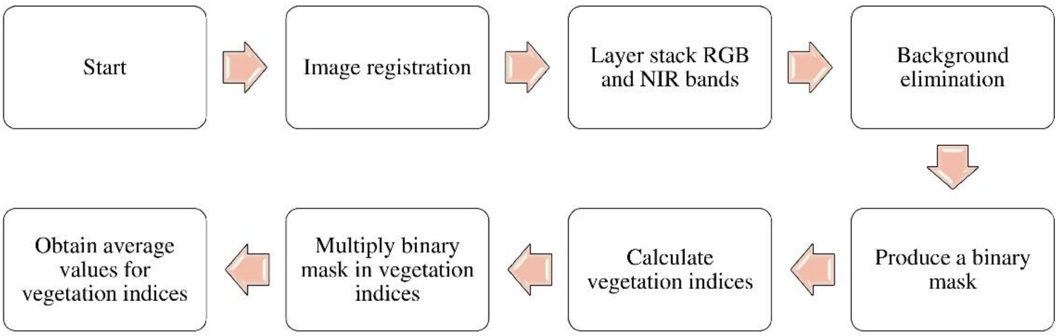

Figure 2. Image processing workflow

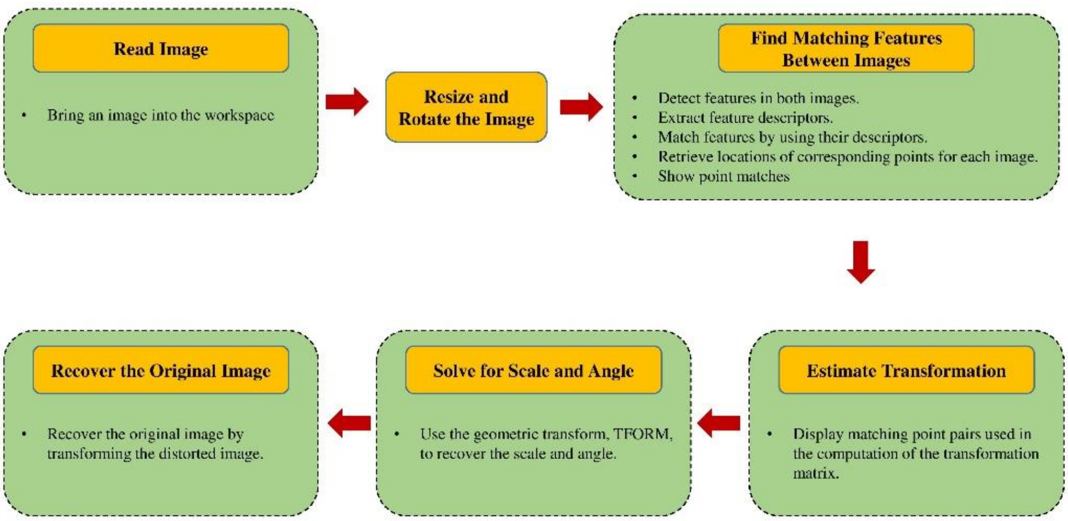

Figure 3. The image registration algorithm

Figure 4. Color image (a) with its corresponding segmentation result of EXG method below (b).

were calculated. Formulas used for calculating vegetation indices are given in Table S1 [suppl]. By multiplying binary mask by vegetation indices, we obtained average values of these indices for each plant. Then, these values were compared with measured data (leaf N content, SPAD and RWC) by using statistical methods.

Statistical analyses

Data collected from both experiments were used to develop regression models between vegetation indices and measured data (leaf N content, SPAD and RWC). It should be noted that this dataset was separated randomly at the ratio of 75:25 for the calibration and validation of the subset, respectively. The fitting quality of regression models was evaluated by adjusted determination coefficient (R^2) (Woebbecke *et al.*, 1995), root mean square error (RMSE) and mean bias error (MBE) (Coelho *et al.*, 2018). RMSE and MBE were given by equations (41) and (42).

$$RMSE = \sqrt{\frac{\sum_{i=1}^{N}(Yobs_i - Yest_i)^2}{N}} \quad (41)$$

$$MBE = \frac{\sum_{i=1}^{N}(Yobs_i - Yest_i)}{N} \quad (42)$$

where: N is the number of data; Yobsi and Yesti are the observed and estimated values of Y, respectively.

When statistical analyses were performed on mean values of the traits, Duncan test was performed to test normal distribution of each treatment. Descriptive statistics were estimated and variance analysis was performed using software IBM SPSS 20.0. Origin Pro 2016 and excel were used to draw Figures.

Results and discussion

Irrigation water applied, plant height, and leaf area index

Fig. 5 shows cumulative irrigation depths for four irrigation treatments. In 2017, the average total amount of irrigation water applied during the entire growing season from planting to harvesting was 483 mm for the control treatment, 457 mm for 80% of field capacity (I_2), 435 mm for 60% of field capacity (I_3), and 402 mm for 40% of field capacity (I_4). In 2018, these figures were 457 mm, 416 mm, 360 mm, and 349 mm for the control and I2, I3 and I4 treatments, respectively. Fig. 6 shows the averages of leaf area and plant height of maize during 2017 and 2018. With different levels of N-fertilizer and irrigation, LAI of maize showed considerable variations over the growth stages; but for all treatments, LAI increased progressively over time, reached its peak within about 40-60 DAS, and, then, began to decrease. Plant height increased progressively over growth stages reaching the highest value upon physiological maturity; however, it varied in response to different N and irrigation levels.

Nitrogen fertilizer applications and leaf nitrogen status

Regression analyses were developed to calibrate SPAD 502 chlorophyll meter by quantifying the relationships between leaf N concentrations and SPAD values for maize production (Fig. 7). Determination

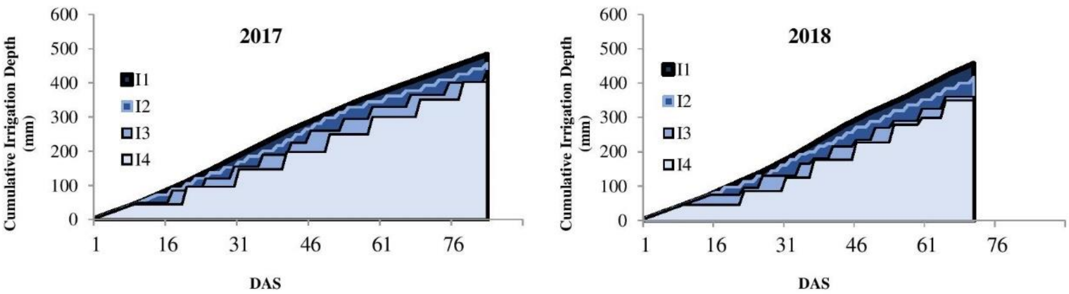

Figure 5. Cumulative irrigation depth for four irrigation treatments: control (I_1); 80 % of field capacity (I_2); 60 % of field capacity (I_3); and 40% of field capacity (I_4).

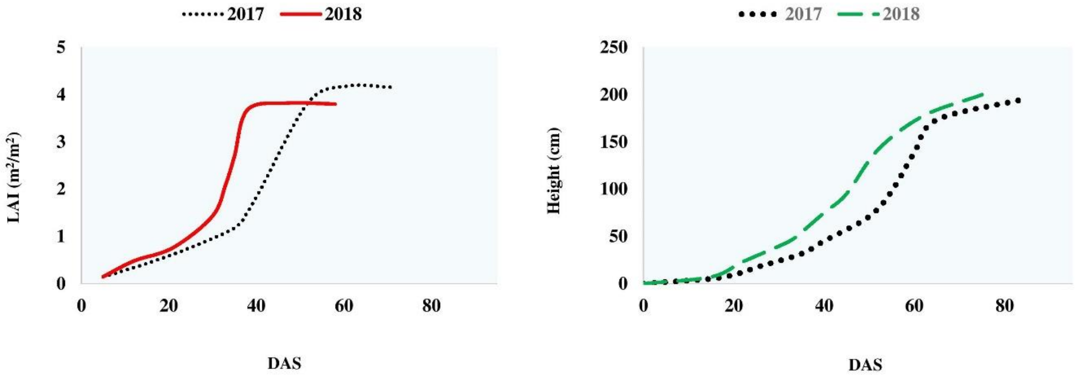

Figure 6. Average of leaf area and plant height of maize during 2017 and 2018

coefficients (R^2) indicated that 78% of the variation in leaf N concentrations were explicated by SPAD reading at each growth stage. Table 2 shows the effects of the N treatments on SPAD values under four irrigation treatments. Results from mean comparisons revealed that SPAD values increased with an increase in the amount of N fertilizer. The same trend was observed for N concentration values not presented in this paper. Several components affect this relationship. In general, leaf greenness increases as soil N availability increases. Throughout the growing season, younger leaves had lower SPAD readings and leaf N concentrations, which increased upon plant growth. Some gradual declines were observed in leaf N concentrations and SPAD values for all N treatments because of the rapid growth before silking. After silking, SPAD values and N contents slightly increased and, then, continued declining (N %). Schepers *et al.* (1992) stated that the stage of crop growth and the time of N application could influence on the SPAD meter readings. The box plot graph of leaf N concentration and SPAD values for data sampling showed that the mentioned trends were observed for data collected in two consecutive years (Fig. 8).

Irrigation traits and relative water content

In Fig. 9, box plot shows RWC rate data used in two years of performing analyses. Plants under I_3 and I_4 treatments usually had a 20-40 % lower RWC than plants receiving adequate water (I_1 and I_2 treatments). In general, leaf RWC was also lower in non-irrigated plants. Regarding the irrigation schedule (Fig. 6), RWC values varied in each day of growth stage. These results are confirmed by several researchers' findings, who stated that leaf RWC was affected by different soil moisture levels, so plants with similar patterns of soil moisture content had similar RWC values (Sangakkara *et al.*, 2010; Zaman *et al.*, 2018).

Relationship between vegetation indices and field measured data (leaf N concentrations, SPAD value and RWC)

In this research, totally 528 images obtained from each RGB and IR cameras were analyzed through image processing and compared with field measured data (leaf N concentrations, SPAD value and RWC). Therefore,

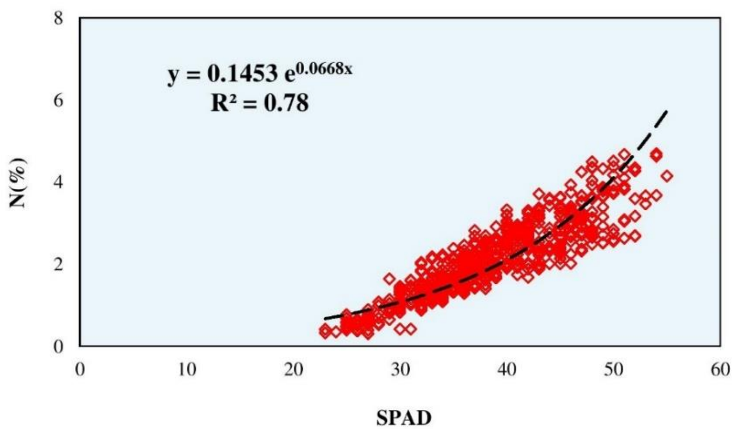

Figure 7. Relationships between leaf N concentrations (N%) and SPAD value at eleven sampling dates for the two experimental years.

Table 2. Mean comparison of main effect of N treatments on SPAD value under four irrigation treatments using Duncan multiple range test.

Treatment [a]		Day after sowing										
Irrigation	Nitrogen	23	27	36	42	43	48	52	55	61	63	71
I_1	N_1	24.333^{i}	30.667^{g}	33.333^{f}	36.333^{e}	37.333^{e}	38.333^{de}	37.667^{e}	39.667^{d}	38.333^{de}	36.667^{e}	35.333^{ef}
	N_2	26.667^{hi}	31.000^{g}	36.333^{e}	38.667^{de}	39.000^{de}	42.000^{cd}	40.333^{d}	43.667^{c}	40.333^{d}	39.333^{de}	38.000^{de}
	N_3	28.333^{gh}	34.667^{f}	44.667^{c}	46.667^{bc}	48.333^{b}	51.000^{ab}	42.333^{cd}	46.333^{bc}	43.667^{c}	42.000^{cd}	40.667^{d}
	N_4	28.333^{gh}	35.667^{ef}	46.667^{bc}	49.667^{b}	51.333^{ab}	54.333^{a}	46.333^{bc}	48.667^{b}	45.667^{c}	43.333^{c}	42.000^{cd}
I_2	N_1	25.667^{hi}	29.667^{g}	33.667^{f}	34.000^{f}	35.000^{ef}	37.667^{e}	34.333^{f}	38.000^{de}	36.667^{e}	33.667^{f}	33.000^{f}
	N_2	26.333^{hi}	31.333^{fg}	35.667^{ef}	38.000^{de}	38.333^{de}	41.333^{d}	38.667^{de}	42.000^{cd}	39.333^{de}	37.667^{e}	37.000^{e}
	N_3	28.667^{gh}	33.667^{f}	43.667^{cd}	46.333^{bc}	47.333^{bc}	51.000^{ab}	41.000^{d}	45.333^{c}	42.000^{cd}	40.333^{d}	39.333^{de}
	N_4	29.333^{gh}	35.333ef	45.667^{c}	50.667^{ab}	50.333^{b}	52.333^{ab}	47.333^{bc}	48.667^{b}	44.333^{c}	45.667^{c}	44.667^{c}
I_3	N_1	25.333^{i}	31.000^{g}	33.333^{f}	34.667^{f}	35.333^{ef}	37.000^{e}	34.667^{f}	37.000^{e}	36.000^{e}	32.667^{f}	31.333^{fg}
	N_2	26.333^{hi}	30.000^{g}	35.333^{ef}	35.333^{ef}	37.333^{e}	40.667^{d}	35.000^{ef}	40.333^{d}	38.333^{de}	34.333^{f}	33.000^{f}
	N_3	26.667^{hi}	33.333f	42.333^{cd}	45.667^{c}	46.000^{bc}	49.000^{b}	40.667^{d}	44.000^{c}	41.333^{d}	38.333^{de}	36.667^{e}
	N_4	27.667^{h}	34.333^{f}	45.000^{c}	50.000^{b}	49.000^{b}	50.667^{ab}	46.667^{bc}	47.333^{bc}	43.667^{c}	45.333^{c}	43.000^{cd}
I_4	N_1	25.000^{i}	28.667^{gh}	32.333^{fg}	32.667^{f}	34.000^{f}	36.000^{e}	32.333^{fg}	35.667^{ef}	34.333^{f}	31.000^{g}	30.000^{g}
	N_2	26.667^{hi}	28.333^{gh}	33.000^{f}	35.333^{ef}	36.000^{e}	39.000^{de}	36.333^{e}	40.000^{d}	37.333^{e}	34.667^{f}	34.000^{f}
	N_3	26.333^{hi}	32.333^{fg}	41.333^{d}	43.333^{c}	45.000^{c}	48.333^{b}	40.333^{d}	42.333^{cd}	40.333^{d}	37.667^{e}	36.667^{e}
	N_4	26.333^{hi}	32.000^{fg}	44.667^{c}	48.333^{b}	48.000^{b}	49.333^{b}	46.000^{bc}	47.000^{bc}	42.333^{cd}	44.333^{c}	42.333^{cd}

[a] I_1, I_2, I_3 and I_4: Irrigation treatments (100, 80, 60, and 40% of field capacity) and N_1, N_2, N_3 and N4: nitrogen treatments (0, 100, 200 and 300 kg N/ha), respectively. Means followed by the same letter are not significantly different at 5% level according to Duncan's Multiple Range Test.

correlations between field measured data and studied vegetation indices (Table S1 [suppl]) were tested to select the best index for estimating field measured data by using regression models.

Details of linear regression models are shown in Table 3. According to R^2, RMSE and MBE values, top 10 performances for linear models were selected based on ranking scores in Table S2 [suppl]. As observed, the best performance results of regression equations between leaf N concentrations, SPAD values, RWC, and vegetation indices were MCARI (R^2=0.590, RMSE=0.714 and MBE=-0.004), CTVI (R^2=0.560, RMSE=0.739 and MBE=-0.004) and CR (R^2=0.530, RMSE=0.768 and MBE=-0.092) for SPAD value; MCARI (R^2=0.430, RMSE=0.653 and MBE=-0.004), HUE (R^2=0.380, RMSE=0.703 and MBE=-0.004) and CTVI (R^2=0.370, RMSE=0.667 and MBE=-0.009) for leaf N concentrations; and TRVI (R^2=450, RMSE=12.750 and MBE=0.007), NDVI (R^2=0.420, RMSE=13.068 and MBE=0.004) and DVI (R^2=0.390, RMSE=13.440 and MBE=0.353) for RWC. In addition, green excess index (EXCESSNIRB) indicated the poorest performance on leaf N concentrations and SPAD value estimations from different stages (R^2=0.0). Also, it should be noted that most regression models did not have an acceptable correlation with RWC values (R^2<0.2).

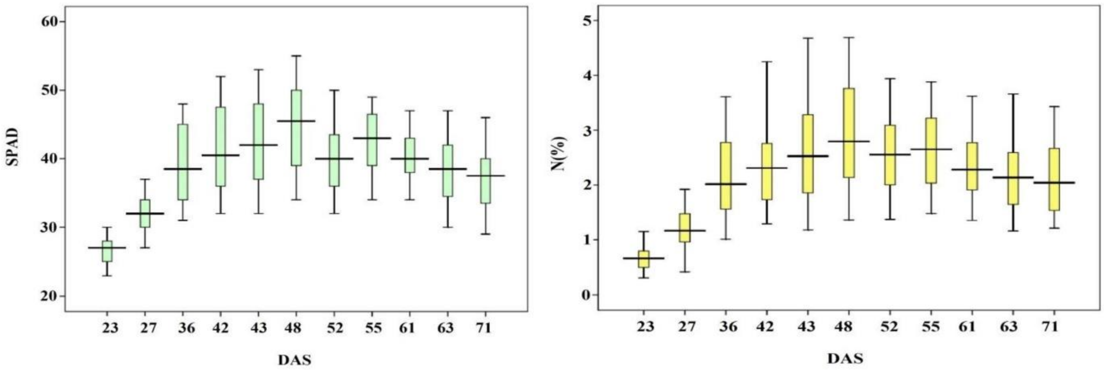

Figure 8. The boxplots of SPAD value and leaf N concentration (N %) for maize 2017 and 2018 samples.

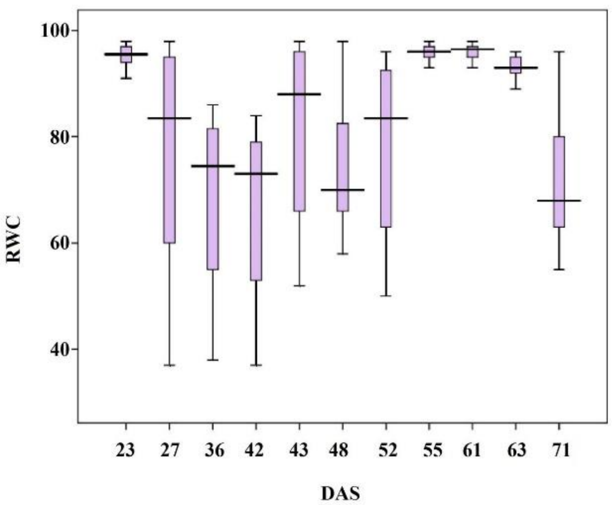

Figure 9. The boxplots of RWC (%) for maize 2017 and 2018 samples.

Our results are in agreement with those of many previous studies examining the use of spectral indices to estimate the N status and RWC content (Clevers & Gitelson, 2013; Schlemmer *et al.*, 2013; Yao *et al.*, 2013). Even though there are differences in the ranking of correlation coefficients in various studies, many of reported differences may not be significant statistically. According to previous studies, for example, MCARI is an index with potential for N fertilizer management (Daughtry *et al.*, 2000; Prey *et al.*, 2018), corresponding well to our study. We found that correlations between MCARI and SPAD values/ leaf N concentration data were consistently among the best spectral indices for data on images taken during 11 days and that MCARI was not sensitive to changes in LAI. Based on studies, N management is very important at the early stages. Thus, it is essential to estimate N status in order to supply appropriate amounts of fertilizer (Zheng *et al.*, 2018). In this regard, our findings showed that the accuracy of results obtained for MCARI was not limited to plant growth stages.

Among studied indices (Table S1 [suppl]), R, G, B and NIR signify the average values of red, green, blue and NIR components of each of RGB and IR images, respectively. Results showed that any combinations of R, G and NIR band formulations had a qualitative relationship with SPAD values and leaf N concentrations. As reported by previous research, R and G components had good relations with chlorophyll contents, but B was poorly related to chlorophyll contents (Yadav *et al.*, 2010; Vesali *et al.*, 2015). Higher chlorophyll contents had a propensity to absorb more energy in the form of light and reduced the light that passed through the leaves (Pérez-Patricio *et al.*, 2018); and lower N con-centrations created higher reflectance percentages in the visible region (Yao *et al.*, 2013). However, Chlorophyll content is dependent on nutritional conditions of plants (*e.g.* leaf N) (Hatfield *et al.*, 2008) and is affected by other stress factors such as water and light (Chaerle & Van Der Straeten, 2000). Therefore, results from SPAD and from N regression models are different.

In this study, indices such as TRVI, NDVI and DVI that used red and NIR regions generally provided more accurate estimates of water status than those operating in the green or blue regions. As shown by previous studies, water treatments were separated in NIR region being strongly influenced by cell structures (Carter, 1991; Schlemmer *et al.*, 2005). The varying water levels altered cell turgidity to create changes in leaf cell structures. Such changes affect energy being absorbed, transmitted, or reflected by NIR (Schlemmer *et al.*, 2005). Water deficit treatments (I_3 and I_4) had higher reflectance values than those of adequate water treatments (I_1 and I_2). N availability have some effects on chlorophyll content and, consequently, on leaf greenness within the visible region. Water stress had a compound effect evidenced by an increase in leaf reflectivity as both N and water stresses increased. Under water-limiting conditions, energy absorption decreases and plant temperature increases, in consequence, an additional increase occurs in reflectance as a plant defence mechanism (Carter, 1991; Schlemmer *et al.*, 2005). An important point is that water stress will not have an immediate impact on chlorophyll content, but will affect the leaf's spectral reflectance (Schlemmer *et al.*, 2005).

Estimation of leaf N concentrations, SPAD value and RWC by a linear model

In order to increase accuracy of estimated measured data, creation of a new regression model was put on the agenda. To build a framework for leaf N concentration, SPAD and RWC estimation, linear regression was used because of its low computational requirements and mathematical simplicity. Although simple linear regression requires lower computational power than multiple regression, results showed that a single variable model was not the best option for measured data estimations. Hence, it was assessed with different combinations of the indices studied in this work. Relationships among the measured data and superior indices were determined by linear regression Equations (43) to (45) by using MCARI, TRVI, NDVI and EVI.

$$N\ (\%) = -1713.24+(-388.56\times TRVI) +(11.41\times NDVI) +(7416.28\times MCARI) +(-2912.81\times EVI) \quad (43)$$

$$SPAD= -14381.73+(3327.32\times TRVI) +(97.61\times NDVI) +(62472.52\times MCARI) +(-24178.2\times EVI) \quad (44)$$

$$RWC= 33654.11+(14097.35\times TRVI) +(-264.13\times NDVI) +(-167107\times MCARI) +(64693.92\times EVI) \quad (45)$$

It was demonstrated that all the proposed indices had acceptable accuracy in terms of leaf N concentration, SPAD value or RWC estimation; especially, the combi-

Table 3. The regression equations between field measured data (leaf N concentrations, SPAD value and RWC), and vegetation indices.

Index	SPAD	N (%)	RWC
BMG	Y= -406.21x - 58.698	Y= -47.601x - 9.2476	Y= -636.29x - 71.008
BMR	Y= 223.42x + 99.153	Y= 28.173x + 9.7868	Y= -14.767x + 77.555
CB	Y= 360.19x - 45850	Y= 43.286x - 5512.5	Y= 54.438x - 6853.9
CIG	Y= -67.187x + 55.447	Y= -8.1671x + 4.2016	Y= 25.623x + 75.162
CR	Y= 99.867x - 12784	Y= 12.13x - 1555.4	Y= 67.432x - 8576.6
CTVI	Y= 1823.4x - 1645	Y= 227.86x - 208.23	Y= 442.31x - 326.86
CVI	Y= 218.99x - 247.53	Y= 26.548x - 32.533	Y= -275.9x + 442.16
DGCI	Y= 161.23x - 35.038	Y= 19.72x - 6.8522	Y= 45.178x + 60.89
DVI	Y= -10937x + 3163.4	Y= -1380.3x + 396.47	Y= 50516x - 14351
EVI	Y= 10963x - 630.4	Y= 1306.7x - 77.52	Y= 23619x - 1360
EXCESSNIRB	Y= 7.7873x + 35.787	Y= 0.7147x + 1.8986	Y= 19.402x + 74.305
EXG	Y= 428.73x - 148.25	Y= 50.822x - 19.994	Y= 507.25x - 139.63
GDR	Y= 183.3x - 133.23	Y= 21.809x - 18.29	Y= 445.97x - 336.75
GDVI	Y= 334.93x - 146.31	Y= 40.117x - 19.993	Y= 759.83x - 338.15
GMR	Y= -214.59x + 14.238	Y= -25.108x - 0.6953	Y= -79.487x + 72.492
GNDVI	Y= 467.26x - 199.5	Y= 56.509x - 26.638	Y= 850.15x - 351.83
GNDVI-NDVI	Y= 1795x - 168.43	Y= 214.48x - 22.578	Y= 2156.6x - 167.29
GOSAVI	Y= 341.32x - 152.19	Y= 42.648x - 21.683	Y= 90.114x + 31.155
GRDVI	Y= 260.65x - 34.359	Y= 32.092x - 6.8277	Y= -37.387x + 92.03
GRVI	Y= 112.87x - 114.59	Y= 13.638x - 16.354	Y= 2.176x + 78.596
GSAVI	Y= 181.33x - 68.865	Y= 21.6x - 10.647	Y= 374.58x - 140.64
HUE	Y= 0.4669x + 1.2	Y= 0.0574x - 2.4484	Y= 0.3256x + 55.4
LIT	Y= 8.383x + 30.21	Y= 0.8978x + 1.2567	Y= 16.162x + 65.193
MCARI	Y= 11358x - 3426.7	Y= 1366.6x - 414.72	Y= 19603x - 5899.3
MGSAVI	Y= 349.64x - 158.15	Y= 39.266x - 19.94	Y= 630.82x - 273.59
MSAVI	Y= 280.66x - 69.664	Y= 35.009x - 11.35	Y= -91.118x + 116.73
MSRG	Y= 149.65x + 9.6929	Y= 18.242x - 1.3694	Y= -172.71x + 115.02
MTVI2	Y= 328.34x - 44.631	Y= 36.578x - 7.1155	Y= -104.09x + 107.97
NDVI	Y= 548.24x - 181.14	Y= 66.37x - 24.445	Y= 1238.6x - 415.11
NDVI-CAM	Y= 105.57x + 55.979	Y= 12.888x + 4.2751	Y= 57.373x + 90.945
NGRDI	Y= 114.7x + 70.838	Y= 14.35x + 6.1861	Y= -20.719x + 75.745
SAT	Y= 82.686x + 5.6574	Y= 10.413x - 1.9952	Y= 72.706x + 52.501
SAVI	Y= 201.15x - 79.083	Y= 23.926x - 11.843	Y= 404.31x - 155.18
SAVI-CAM	Y= -1281x - 95.685	Y= -153.8x - 13.968	Y= 210.8x + 103.66
SR	Y= 121.83x - 116.73	Y= 14.613x - 16.477	Y= 263.9x - 255.13
TGI	Y= 48.176x + 22.662	Y= 6.0274x + 0.1596	Y= -8.7018x + 84.447
TRVI	Y= 1036.9x - 959.01	Y= 125.6x - 118.68	Y= 2420.8x - 2247.8
TVI	Y= 19.45x - 54.524	Y= 2.3923x - 9.3004	Y= -1.2676x + 87.626
VAL	Y= 281.56x - 209	Y= 33.471x - 27.28	Y= -24.1x + 102.75
YY	Y= 558.15x - 9105.9	Y= 67.908x - 1110.4	Y= -169.37x + 2856.5

Table 4. Performance results of multiple linear regression model between field measured data (leaf N concentrations, SPAD value and RWC), and vegetation indices.

	R^2	RMSE	MBE
SPAD	0.91	2.06	0.00000
N	0.60	0.50	0.00065
RWC	0.90	5.54	0.00000

RWC: relative water content. RMSE: root mean square error. MBE: mean bias error.

nation of all indices provided more accuracy to most of the previous single variable regression models (Table 3). Table 4 gives the results of predicting measured data from multiple linear regression model with the measured data. As observed, R^2 values were 0.91, 0.60 and 0.90 for SPAD value, leaf N concentration and RWC estimation, respectively.

In summary, this study showed that low-cost modified consumer-grade cameras is satisfactory. These results can be useful and applicable to monitoring the leaf N concentrations, SPAD values and RWC, and represent an appropriate tool to support precision exercised in agriculture.

References

Ahmadi K, 2017. Annual agricultural statistics. Ministry of Jihad-e-Agriculture of Iran. https://maj.ir/

Akhavan S, Mousabeygi F, Peel MC, 2018. Assessment of eight reference evapotranspiration (ETo) methods considering Köppen climate class in Iran. Hydrol Sci J 63(10): 1468-1481. https://doi.org/10.1080/02626667.2018.1513654

Ballester C, Jiménez-Bello MA, Castel JR, Intrigliolo DS, 2013. Usefulness of thermography for plant water stress detection in citrus and persimmon trees. Agr For Meteorol 168: 120-129. https://doi.org/10.1016/j.agrformet.2012.08.005

Cao Q, Miao Y, Huang S, Wang H, Khosla R, Jiang R, 2013a. Estimating rice nitrogen status with the Crop Circle multispectral active canopy sensor. Precis Agr 13: 95-101. https://doi.org/10.1016/j.fcr.2013.08.005

Cao Q, Miao Y, Wang H, Huang S, Cheng S, Khosla R, Jiang R, 2013b. Non-destructive estimation of rice plant nitrogen status with Crop Circle multispectral active canopy sensor. Field Crops Res 154: 133-144. https://doi.org/10.1016/j.fcr.2013.08.005

Cao Q, Miao Y, Feng G, Gao X, Li F, Liu B, *et al.*, 2015. Active canopy sensing of winter wheat nitrogen status: An evaluation of two sensor systems. Comput Electron Agr 112: 54-67. https://doi.org/10.1016/j.compag.2014.08.012

Cao Q, Miao Y, Wang H, Huang S, Cheng S, Khosla R, Jiang R, 2018. Multi-focus fusion technique on low-cost camera images for canola phenotyping. Sensors 18(6): 1887. https://doi.org/10.3390/s18061887

Carter GA, 1991. Primary and secondary effects of water content on the spectral reflectance of leaves. Am J Bot 78(7): 916-924. https://doi.org/10.1002/j.1537-2197.1991.tb14495.x

Chaerle L, Van Der Straeten D, 2000. Imaging techniques and the early detection of plant stress. Trends Plant Sci 5(11): 495-501. https://doi.org/10.1016/S1360-1385(00)01781-7

Clevers JG, Gitelson AA, 2013. Remote estimation of crop and grass chlorophyll and nitrogen content using red-edge bands on Sentinel-2 and-3. Int J Appl Earth Observ Geoinform 23: 344-351. https://doi.org/10.1016/j.jag.2012.10.008

Coelho AP, Rosalen DL, Faria RT, 2018. Vegetation indices in the prediction of biomass and grain yield of white oat under irrigation levels. Pesqu Agropec Trop 48(2): 109-117. https://doi.org/10.1590/1983-40632018v4851523

Daughtry C, 1990. Direct measurements of canopy structure. Remote Sens Rev 5(1): 45-60. https://doi.org/10.1080/02757259009532121

Daughtry CS, Walthall CL, Kim MS, De Colstoun EB, McMurtrey Iii JE, 2000. Estimating corn leaf chlorophyll concentration from leaf and canopy reflectance. Remote Sens Environ 74(2): 229-239. https://doi.org/10.1016/S0034-4257(00)00113-9

de Oca AM, Arreola L, Flores A, Sanchez J, Flores G, 2018. Low-cost multispectral imaging system for crop monitoring. Int Conf on Unmanned Aircraft Systems (ICUAS). IEEE, Dallas (TX), USA. https://doi.org/10.1109/ICUAS.2018.8453426

Dhillon R, Francisco RO, Roach J, Upadyaya S, Delwiche M, 2014. A continuous leaf monitoring system for precision irrigation management in orchard crops. Tarım Makinaları Bilimi Dergisi 10(4): 267-272.

Dumas JB, 1831. Procedes de l'analyse organique. Ann Chimie Phys 47: 198-205.

García CE, Montero D, Chica HA, 2017. Evaluation of a NIR camera for monitoring yield and nitrogen effect in sugarcane. Agronomía Colombiana 35(1): 82-91. https://doi.org/10.15446/agron.colomb.v35n1.60852

Geelen B, Spooren N, Tack K, Lambrechts A, Jayapala M, 2017. System-level analysis and design for RGB-NIR CMOS camera. Photonic Instrum Eng IV, Int Soc for Optics and Photonics. https://doi.org/10.1117/12.2250852

Gitelson AA, Kaufman YJ, Merzlyak MN, 1996. Use of a green channel in remote sensing of global vegetation from EOS-MODIS. Remote Sens Environ 58 (3): 289-298. https://doi.org/10.1016/S0034-4257(96)00072-7

Gitelson AA, Vina A, Ciganda V, Rundquist DC, Arkebauer TJ, 2005. Remote estimation of canopy chlorophyll content in crops. Geophys Res Lett 32(8). https://doi.org/10.1029/2005GL022688

Guo JH, Wang X, Meng ZJ, Zhao CJ, Yu ZR, Chen LP, 2008. Study on diagnosing nitrogen nutrition status of corn using Greenseeker and SPAD meter. Plant Nutr Fertil Sci 14(1): 43-47.

Hatfield JL, Gitelson AA, Schepers JS, Walthall CL, 2008. Application of spectral remote sensing for agronomic decisions. Agron J 100(S3): S117-S131. https://doi.org/10.2134/agronj2006.0370c

Hawkins JA, Sawyer JE, Barker DW, Lundvall JP, 2007. Using relative chlorophyll meter values to determine nitrogen application rates for corn. Agron J 99(4): 1034-1040. https://doi.org/10.2134/agronj2006.0309

Huete A, Didan K, Miura T, Rodriguez EP, Gao X, Ferreira LG, 2002. Overview of the radiometric and biophysical performance of the MODIS vegetation indices. Remote Sens Environ 83(1-2): 195-213. https://doi.org/10.1016/S0034-4257(02)00096-2

Hunt Jr ER, Doraiswamy PC, McMurtrey JE, Daughtry CS, Perry EM, Akhmedov B, 2013. A visible band index for remote sensing leaf chlorophyll content at the canopy scale. Int J Appl Earth Observ Geoinform 21: 103-112. https://doi.org/10.1016/j.jag.2012.07.020

Inoue Y, Sakaiya E, Zhu Y, Takahashi W, 2012. Diagnostic mapping of canopy nitrogen content in rice based on hyperspectral measurements. Remote Sens Environ 126: 210-221. https://doi.org/10.1016/j.rse.2012.08.026

Kaushal SS, Groffman PM, Band LE, 2011. Tracking nonpoint source nitrogen pollution in human-impacted watersheds. Environ Sci Technol 45(19): 8225-8232. https://doi.org/10.1021/es200779e

Khan Z, Rahimi-Eichi V, Haefele S, Garnett T, Miklavcic SJ, 2018. Estimation of vegetation indices for high-throughput phenotyping of wheat using aerial imaging. Plant Methods 14(1): 20. https://doi.org/10.1186/s13007-018-0287-6

Kim Y, Glenn DM, Park J, Ngugi HK, Lehman BL, 2011. Hyperspectral image analysis for water stress detection of apple trees. Comput Electron Agr 77(2): 155-160. https://doi.org/10.1016/j.compag.2011.04.008

Kjeldahl JG, 1883. Neue methode zur bestimmung des stickstoffs in organischen körpern. Fresenius' Journal of Analytical Chemistry 22(1): 366-382. https://doi.org/10.1007/BF01338151

Le Maire G, Francois C, Dufrene E, 2004. Towards universal broad leaf chlorophyll indices using PROSPECT simulated database and hyperspectral reflectance measurements. Remote Sens Environ 89(1): 1-28. https://doi.org/10.1016/j.rse.2003.09.004

Maki M, Ishiahra M, Tamura M, 2004. Estimation of leaf water status to monitor the risk of forest fires by using remotely sensed data. Remote Sens Environ 90(4): 441-450. https://doi.org/10.1016/j.rse.2004.02.002

Monno Y, Teranaka H, Yoshizaki K, Tanaka M, Okutomi M, 2019. Single-sensor RGB-NIR imaging: High-quality system design and prototype implementation. IEEE Sensor J 19(2): 497-507. https://doi.org/10.1109/JSEN.2018.2876774

Muñoz-Huerta RF, Guevara-Gonzalez RG, Contreras-Medina LM, Torres-Pacheco I, Prado-Olivarez J, Ocampo-Velazquez RV, 2013. A review of methods for sensing the nitrogen status in plants: advantages, disadvantages and recent advances. Sensors 13(8): 10823-10843. https://doi.org/10.3390/s130810823

Onoyama H, Ryu C, Suguri M, Iida M, 2015. Nitrogen prediction model of rice plant at panicle initiation stage using ground-based hyperspectral imaging: growing degree-days integrated model. Precis Agr 16(5): 558-570. https://doi.org/10.1007/s11119-015-9394-9

Pérez-Patricio M, Camas-Anzueto JL, Sanchez-Alegría A, Aguilar-González A, Gutiérrez-Miceli F, Escobar-Gómez E, *et al.*, 2018. Optical method for estimating the chlorophyll contents in plant leaves. Sensors 18(2): 650. https://doi.org/10.3390/s18020650

Perry Jr CR, Lautenschlager LF, 1984. Functional equivalence of spectral vegetation indices. Remote Sens Environ 14(1-3): 169-182. https://doi.org/10.1016/0034-4257(84)90013-0

Prasertsak A, Fukai S, 1997. Nitrogen availability and water stress interaction on rice growth and yield. Field Crops Res 52(3): 249-260. https://doi.org/10.1016/S0378-4290(97)00016-6

Prey L, Von Bloh M, Schmidhalter U, 2018. Evaluating RGB imaging and multispectral active and hyperspectral passive sensing for assessing early plant vigor in winter wheat. Sensors 18(9): 2931. https://doi.org/10.3390/s18092931

Pu R, Ge S, Kelly NM, Gong P, 2003. Spectral absorption features as indicators of water status in coast live oak (*Quercus agrifolia*) leaves. Int J Remote Sens 24(9): 1799-1810. https://doi.org/10.1080/01431160210155965

Putra BT, Soni P, 2017. Evaluating NIR-Red and NIR-Red edge external filters with digital cameras for assessing vegetation indices under different illumination. Infrared Phys Technol 81: 148-156. https://doi.org/10.1016/j.infrared.2017.01.007

Ritchie GL, Sullivan DG, Perry CD, Hook JE, Bednarz CW, 2008. Preparation of a low-cost digital camera system for remote sensing. Appl Eng Agr 24(6): 885-894. https://doi.org/10.13031/2013.25359

Romano G, Zia S, Spreer W, Sanchez C, Cairns J, Araus JL, Müller J, 2011. Use of thermography for high throughput phenotyping of tropical maize adaptation in water stress. Comput Electron Agr 79(1): 67-74. https://doi.org/10.1016/j.compag.2011.08.011

Rouse JW, Hass RH, Schell JA, 1975. Measuring foriage production of grazing units from LANDSAT MSS data. Proc 10th Int Symp on Remote Sensing of Environment, Michigan, Ann Arbor (USA).

Saberioon MM, Amin MS, Gholizadeh A, Ezri MH, 2014. A review of optical methods for assessing nitrogen contents during rice growth. Appl Eng Agr 30(4): 657-669. https://doi.org/10.13031/aea.30.10478

Samseemoung G, Soni P, Jayasuriya HP, Salokhe VM, 2012. Application of low altitude remote sensing (LARS) platform for monitoring crop growth and weed infestation in a soybean plantation. Precis Agr 13(6): 611-627. https://doi.org/10.1007/s11119-012-9271-8

Sangakkara UR, Amarasekera P, Stamp P, 2010. Irrigation regimes affect early root development, shoot growth and yields of maize (Zea mays L.) in tropical minor seasons. Plant Soil Environ 56(5): 228-234.

Schepers JS, Francis DD, Vigil M, Below FE, 1992. Comparison of corn leaf nitrogen concentration and chlorophyll meter readings. Commun Soil Sci Plant Anal 23(17-20): 2173-2187. https://doi.org/10.1080/00103629209368733

Schlemmer MR, Francis DD, Shanahan JF, Schepers JS, 2005. Remotely measuring chlorophyll content in corn leaves with differing nitrogen levels and relative water content. Agron J 97(1): 106-112. https://doi.org/10.2134/agronj2005.0106

Schlemmer M, Gitelson A, Schepers J, Ferguson R, Peng Y, Shanahan J, Rundquist D, 2013. Remote estimation of nitrogen and chlorophyll contents in maize at leaf and canopy levels. Int J Appl Earth Observ Geoinform 25: 47-54. https://doi.org/10.1016/j.jag.2013.04.003

Sripada RP, Heiniger RW, White JG, Meijer AD, 2006. Aerial color infrared photography for determining early in-season nitrogen requirements in corn. Agron J 98(4): 968-977. https://doi.org/10.2134/agronj2005.0200

Swain KC, Thomson SJ, Jayasuriya HP, 2010. Adoption of an unmanned helicopter for low-altitude remote sensing to estimate yield and total biomass of a rice crop. T ASAE 53(1): 21-27. https://doi.org/10.13031/2013.29493

Tucker CJ, 1979. Red and photographic infrared linear combinations for monitoring vegetation. Remote Sens Environ 8(2): 127-150. https://doi.org/10.1016/0034-4257(79)90013-0

Vesali F, Omid M, Kaleita A, Mobli H, 2015. Development of an android app to estimate chlorophyll content of corn leaves based on contact imaging. Comput Electron Agr 116: 211-220. https://doi.org/10.1016/j.compag.2015.06.012

Woebbecke DM, Meyer GE, Von Bargen K, Mortensen DA, 1995. Shape features for identifying young weeds using image analysis. T ASAE 38(1): 271-281. https://doi.org/10.13031/2013.27839

Yadav SP, Ibaraki Y, Gupta SD, 2010. Estimation of the chlorophyll content of micropropagated potato plants using RGB based image analysis. Plant Cell Tissue Organ Cult 100(2): 183-188. https://doi.org/10.1007/s11240-009-9635-6

Yang C, Westbrook JK, Suh CP, Martin DE, Hoffmann WC, Lan Y, *et al.*, 2014. An airborne multispectral imaging system based on two consumer-grade cameras for agricultural remote sensing. Remote Sens 6(6): 5257-5278. https://doi.org/10.3390/rs6065257

Yang Z, Willis P, Mueller R, 2008. Impact of band-ratio enhanced AWIFS image to crop classification accuracy. Pecora 17 - The Future of Land Imaging Going Operational Denver: 18-20.

Yao X, Yao X, Jia W, Tian Y, Ni J, Cao W, Zhu Y, 2013. Comparison and intercalibration of vegetation indices from different sensors for monitoring above-ground plant nitrogen uptake in winter wheat. Sensors 13(3): 3109-3130. https://doi.org/10.3390/s130303109

Zaman NK, Abdullah MY, Othman S, Zaman NK, 2018. Growth and physiological performance of aerobic and lowland rice as affected by water stress at selected growth stages. Rice Sci 25(2): 82-93. https://doi.org/10.1016/j.rsci.2018.02.001

Zhang JH, Ke WA, Bailey JS, Ren-Chao WA, 2006. Predicting nitrogen status of rice using multispectral data at canopy scale1. Pedosphere 16(1): 108-117. https://doi.org/10.1016/S1002-0160(06)60032-5

Zhang J, Blackmer AM, Blackmer TM, 2008. Differences in physiological age affect diagnosis of nitrogen deficiencies in cornfields. Pedosphere 18(5): 545-553. https://doi.org/10.1016/S1002-0160(08)60048-X

Zhang J, Yang C, Song H, Hoffmann WC, Zhang D, Zhang G, 2016. Evaluation of an airborne remote sensing platform consisting of two consumer-grade cameras for crop identification. Remote Sens 8(3): 257. https://doi.org/10.3390/rs8030257

Zheng H, Cheng T, Li D, Zhou X, Yao X, Tian Y, *et al.*, 2018. Evaluation of RGB, color-infrared and multispectral images acquired from unmanned aerial systems for the estimation of nitrogen accumulation in rice. Remote Sens 10(6): 824. https://doi.org/10.3390/rs10060824

Ziadi N, Brassard M, Bélanger G, Claessens A, Tremblay N, Cambouris AN, *et al.*, 2008. Chlorophyll measurements and nitrogen nutrition index for the evaluation of corn nitrogen status. Agron J 100(5): 1264-1273. https://doi.org/10.2134/agronj2008.0016